CIRP Journal of Manufacturing Science and Technology 64 (2026) 65–78

Contents lists available at ScienceDirect

CIRP Journal of Manufacturing Science and Technology

journal homepage: www.elsevier.com/locate/cirpj

An approach for integrating performance evaluation and environmental sustainability assessment for hybrid additive-subtractive manufacturing

Paolo C. Priarone [a], Maria Chiara Magnanini [b,*]

[a] Politecnico di Torino, Department of Management and Production Engineering, Corso Duca degli Abruzzi 24, Torino 10129, Italy
[b] Politecnico di Milano, Department of Mechanical Engineering, Via La Masa 1, Milano 20156, Italy

ARTICLE INFO

Keywords:
Manufacturing systems
Energy efficiency
Additive manufacturing
Machining
Stochastic modeling

ABSTRACT

Manufacturing systems that integrate additive and subtractive unit processes within a unified workflow aim to leverage the respective strengths of each technology. This study presents a modeling framework for assessing the environmental performance of hybrid manufacturing systems, explicitly accounting for stochastic system-level dynamics such as blocking (when an upstream process is forced to stop because the downstream buffer is full) and starvation (when a downstream process remains idle because the upstream buffer is empty). The model is applied to a case study combining wire arc additive manufacturing and 5-axis CNC milling, under three different process scenarios and multiple system configurations. Increasing buffer capacity reduces idle states and enables the system to operate closer to its maximum throughput, at the cost of higher work in progress. As productivity increases, specific energy consumption and emissions per part decrease. These findings extend traditional process-level models to a multi-stage context, highlighting the importance of system integration. Overall, the study demonstrates that applying the proposed model can improve energy efficiency and carbon footprint by jointly considering process strategies and system configuration, supporting more informed, sustainability-oriented design and planning decisions.

1. Introduction

The broad push towards sustainability, understood in its most comprehensive sense according to the so-called 'triple bottom line', presents manufacturers with significant challenges in configuring and operating their manufacturing systems. Operating a process optimally requires identifying the appropriate parameters not only in terms of quality and cost, but also with regard to resource efficiency [12]. Recent research in manufacturing increasingly focuses on energy efficiency, reconfigurability, and sustainable production, driven by economic as well as environmental pressures. This progress is underpinned by the convergence of digital technologies, optimization methods, and smart manufacturing concepts.

In the literature, researchers have been focusing on some major trends, mainly treating system configuration, process operation, and environmental sustainability as independent pillars. However, some relevant examples, coming from different manufacturing contexts, can be analyzed in light of the current scientific landscape. AlGeddawy & ElMaraghy [2] introduced a methodology for designing manufacturing systems for sustainability, proposing to embed energy considerations early in the system design phase. Their framework links process energy models with production planning to reduce energy consumption proactively. Similarly, well-established research streams focus on energy-efficient control policies based on time-based policies, as in Frigerio & Matta [17] and Tan et al. [46]. Then, introducing a novel approach that laid the groundwork for the one presented here, Wójcicki et al. [49] modeled energy demand in machining systems using a two-machine generalized threshold approach, enabling more accurate energy control and supporting energy-conscious production strategies. Similarly, Loffredo et al. [31] applied reinforcement learning (RL) to dynamically control parallel machines, demonstrating real-time energy savings through data-driven control policies. In this case, less emphasis is placed on system configuration, as the focus is on operational policies. Reconfigurable manufacturing systems (RMS) are critical for meeting evolving production demands with minimal environmental impact. Yelles-Chaouche et al. [50] reviewed optimization approaches in RMS, categorizing methods for layout design, resource allocation, and system evolution, while highlighting gaps in sustainable metrics integration. Khezri et al. [28] further advanced this by developing multi-objective optimization models for sustainable RMS (SRMS), targeting process

* Corresponding author.
E-mail address: mariachiara.magnanini@polimi.it (M.C. Magnanini).

https://doi.org/10.1016/j.cirpj.2025.11.009
Received 18 July 2025; Received in revised form 25 October 2025; Accepted 23 November 2025
Available online 3 December 2025
1755-5817/© 2025 The Author(s). This is an open access article under the CC BY-NC-ND license (http://creativecommons.org/licenses/by-nc-nd/4.0/).

plan generation that balances cost, time, and energy.

In novel manufacturing processes, understanding the relationship between configuration choices and operational policies is crucial for informed decision-making. When it comes to additive manufacturing (AM), this technology has received increasing attention for its potential to optimize material and energy use. Karimi et al. [26] proposed an energy-aware scheduling model for AM to minimize power usage while maintaining throughput. Ma et al. [33] analyzed energy consumption distribution in AM processes, highlighting the importance of machine parameters and build strategies. A comprehensive review by May & Psarommatis [35] synthesized current findings and proposed a framework for maximizing energy efficiency in AM, emphasizing the need for standardized metrics and lifecycle assessments to guide future developments. Nonetheless, AM systems must be evaluated within the broader manufacturing workflow, as they often require mandatory post-processing and finishing operations, particularly for metal components, to meet the strict application-specific requirements [32]. To this end, hybrid manufacturing approaches combine AM processes, such as Powder Bed Fusion (PBF) or Directed Energy Deposition (DED), for near-net-shape production, with conventional techniques, such as CNC machining, to achieve satisfactory precision and surface quality while offering a promising route to functional, energy-efficient production. Strong et al. [45] examined the integration of AM into traditional supply chains, identifying challenges and opportunities in logistics, production control, and quality assurance. Smith et al. [44] provided a more recent technical perspective on hybrid metal additive/subtractive machine tools, detailing use cases and control challenges.

Despite the growing body of research, a gap remains in practical methodologies that simultaneously integrate system configuration, process strategies, and environmental metrics for hybrid additive-subtractive manufacturing. Among the different systems which have been developed over the last couple of decades (as reviewed in [43]), a hybrid manufacturing approach based on a Wire Arc Additive Manufacturing (WAAM) process followed by 5-axis CNC milling has been considered in this study. This combination of processes has been gaining momentum, since WAAM enables the extension of layer-by-layer fabrication benefits to medium-to-large parts with deposition rates far higher than powder-bed technologies. However, the WAAM limitations in terms of quality and accuracy of the as-deposited features typically require a machining process afterwards [20,42]. The goal of this work is to investigate the environmental assessment resulting from the joint analysis of system configuration and process operation. A methodology is proposed to contribute to the development of strategic decision support tools designed to provide feedback on the integrated choice of the process variables and system configuration. An analytical model for performance evaluation is used, due to the fast computational time. For the sustainability assessment, different empirical models are exploited, according to the state-of-the-art literature, and Cumulative Energy Demand (CED) and equivalent carbon dioxide emissions (CO_2) are the selected metrics to quantify the environmental stress. The remainder of the paper is structured as follows: Section 2 outlines the modeling framework, including the characterization of individual unit processes and the formulation of system-level performance and environmental assessment models. Section 3 introduces the case study, based on WAAM followed by CNC milling, illustrating the applicability of the proposed methodology across different process scenarios. Section 4 discusses the results, with particular emphasis on system dynamics and sustainability trade-offs. Finally, Section 5 concludes the study and outlines directions for future research.

2. Framework and methods

In hybrid approaches, both the additive manufacturing (AM) and the subtractive manufacturing (SM) technologies can be implemented in a single machine or manufacturing cell. Highly-flexible solutions have already been established, based either on single/multiple robotic systems or CNC platforms [16,4]. When a single hybrid machine is chosen, and one component is processed (or even repaired) at a time by following sequential process phases (e.g., [8]), any disruptive stoppage in the additive operation would cause a delay in the subtractive operation. Conversely, any disruptive stoppage in the subtractive operation would prevent the next additive operation from beginning.

Alternatively, the same integrated manufacturing approach can be implemented using two distinct and separate machines (Fig. 1). This case represents a typical scenario for companies aiming to update and/or flexibly reconfigure their production lines by adding one or more AM machines to the already available equipment. Compared to the previous case, production planning becomes more complex due to the need to manage internal logistics and the transfer of semi-manufactured parts from the AM machine to the SM one. The input process parameters (for both AM and SM) and the buffer configuration must be defined as a function of the geometrical product specifications, the production targets, and the goal of maximizing the overall system performance in terms of productivity and sustainability. The framework proposed in Fig. 1 is based on the characterization of each unit process (detailed in Section 2.1), which provides the needed information from the manufacturing system. Then, to develop strategic decision support tools at the system level, two separate – but closely connected – steps of performance evaluation (described in Section 2.2) and environmental sustainability evaluation (Section 2.3) are carried out.

2.1. Unit-process characterization

In order to apply the framework proposed in Fig. 1, the characterization of each unit process has to be performed. The performance evaluation requires (*i*) the cycle time for the single part manufacturing (CT^k), (*ii*) the mean time to failure ($MTTF^k$), (*iii*) the mean time to repair ($MTTR^k$), for either $k =$ AM or SM, and (*iv*) the buffer size (N). Furthermore, for the environmental sustainability assessment, (*i*) the energy consumption (E^k_{CT}) and/or the power demanded by each machine during CT^k, including all the auxiliary equipment, as well as (*ii*) the consumption rate ($\dot{q}^k_j$) of all the j-th consumable resources must be obtained. This is the minimum condition necessary to perform the analysis, which is, however, simplified by the digital technologies of Industry 4.0 [13], as the use of highly sensorised, vertically- and horizontally-integrated machines enables the acquisition of a complete set of data [19].

2.1.1. Modeling of energy and power requirements

The average power demanded by any manufacturing equipment, $\overline{P^k_P}$ (in kW), can be computed on a per-part basis as the ratio between the electrical energy consumption, E^k_{CT} (in kWh), and CT^k (in h), according to Eq. 1,

$$\overline{P^k_P} = \frac{E^k_{CT}}{CT^k} = \frac{\int_{t_0}^{t_1} P^k(t)\,dt}{CT^k} \tag{1}$$

where the total cycle time, CT^k, from the beginning (t_0) to the end (t_1) of the operation, shall include both the productive and non-productive times associated to the production of a single part. Eq. 1 has a general validity. Nevertheless, at the unit-process level, empirical approaches have already proven their effectiveness in modeling the (specific) energy requirements while varying the process variables (e.g., [25]), and can therefore be used for quantifying and/or predicting E^k_{CT}.

With reference to the hybrid manufacturing approach here considered, an example of data acquired when manufacturing a near-net-shape part by means of a WAAM unit process is shown in Fig. 2. The total power-versus-time profile includes all the contributions due to the deposition system, the positioning system, and all the auxiliary systems, such as the cooling and smoke evacuation units [39]. The periodic

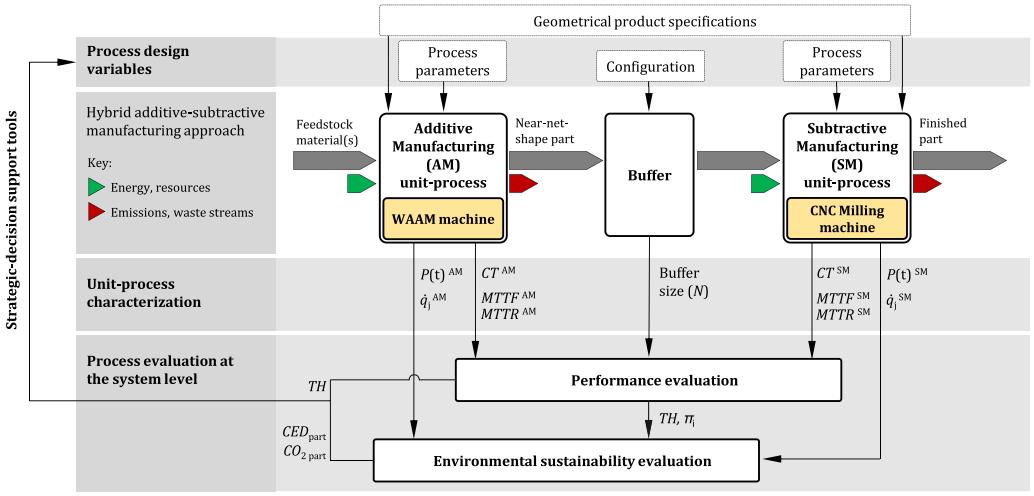

Fig. 1. Framework for integrating performance evaluation and sustainability assessment in hybrid additive-subtractive manufacturing.

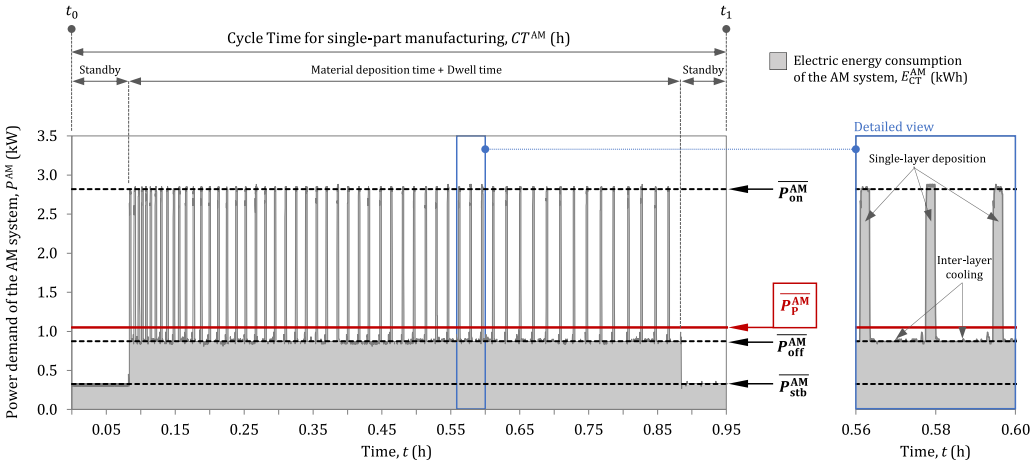

Fig. 2. Power demand versus time results for a WAAM system. The example refers to a thin-walled structure made of 55 overlapped layers, which were deposited under a Wire Feed Speed (*WFS*) of 3 m/min and a Travel Speed (*TS*) of 0.5 m/min.

stepwise shape of the power-versus-time curve allows identifying three main phases, which are related to the time for the active material deposition (i.e., the arc-on time, t_{on}), the dwell time for interlayer cooling (i.e., the arc-off time, t_{off}), and the standby time (t_{stb}), on a per-part basis, for substrate loading and part unloading. Every phase of this WAAM process requires an almost-constant power demand. Therefore, Eq. 1 can be here approximated as per Eq. 2,

$$\overline{P_{p}^{AM}} = \frac{E_{CT}^{AM}}{CT^{AM}} \cong \frac{\overline{P_{on}^{AM}} \cdot t_{on} + \overline{P_{off}^{AM}} \cdot t_{off} + \overline{P_{stb}^{AM}} \cdot t_{stb}}{CT^{AM}} \quad (2)$$

where $\overline{P_{on}^{AM}}$, $\overline{P_{off}^{AM}}$, and $\overline{P_{stb}^{AM}}$ (in kW) are the average power demand values during arc-on time, arc-off time and standby time, respectively (as labeled in Fig. 2).

The average power levels and times vary as a function of both the geometry of the part being produced and the process parameters [9]. The power levels can be measured during a preliminary machine characterization, whereas the active deposition time and dwell time can be obtained from the CAM software which defines the deposition strategies. Therefore, if all the power levels and the process times are known, the electrical energy consumption in isolation of the WAAM unit process can be estimated a priori. Moreover, unit-process models based on the Specific Energy Consumption (*SEC*) – that is, the amount of energy required by the process/equipment to manufacture a unit of mass of a given material – have been already established for machining [25,30], and further applied to other manufacturing processes in which the constant power requirement of the machine equipment dominates the total energy consumption. Thus, if the *SEC* values are available for the given unit process as the configuration changes, and if the mass of material to be processed is known, the $\overline{P_{p}^{k}}$ value can also be estimated using this approach. For the sake of clarification, examples of data collection and/or modeling alternatives will be provided during the discussion of the case study (Section 3).

2.2. Performance evaluation

The performance evaluation allows estimating (or predicting) the productivity indicators according to the variation of the process and configuration parameters. The productivity indicators include (*i*) the system throughput, *TH*, which is the expected number of parts produced by the manufacturing system within the time unit, (*ii*) the work-in-progress, *WIP*, which is the average content of the inter-operational buffer in terms of parts, and (*iii*) the probability π^{k} that each *k*-th unit process is in a certain production state in a given time unit. A production state can be defined as an operational mode which depends on both the behavior of the single unit process and the interaction between unit processes in a given configuration. When the additive-subtractive manufacturing approach is performed by exploiting two separate unit

processes, the overall system behavior depends on the joint dynamics of the two machines, which are partially decoupled by the inter-operational buffer. In fact, when the buffer is nor full or empty, the two unit processes can manage the parts flowing in the system without influencing each other from the viewpoint of the operational mode. If an unexpected stoppage occurs in the AM unit process, the buffer may start to decrease. Then, if the stoppage of the AM unit process continues for some time, the buffer will become empty. Hence, the downstream SM unit process will not be able to manufacture parts anymore, as no near-net-shape parts are available. As a consequence, the subtractive unit process will be starved (in the operational mode of '*starvation*'). Similarly, when an unexpected stoppage occurs in the SM unit process, the buffer may start to increase since no parts are processed by the subtractive stage anymore. Then, if the stoppage of the SM unit process continues for some time, the buffer will become full. Hence, the upstream AM unit process will be blocked (in the operational mode of '*blocking*'), as no parts can be downloaded in the downstream buffer.

Since stoppages may be seen as stochastic events characterized by a statistical distribution, the system performance cannot be known a priori due to the effects of variability and propagation of variability among the stages. Different methods can be used to compute the system key performance indicators (KPIs), as data-driven methods [51], and model-based methods [29]. A model-based methodology is used in this research, which grounds on a set of analytical equations to estimate the performance indicators without severe computing effort, as in Discrete Event Simulation (DES) [37], or extensive data, as in approaches involving Neural Networks [23] or Supervised Learning [27]. Obviously, according to the specific context, all methods can be used as far as they provide the same KPIs. The here-used methodology is based on the model for two-stage manufacturing lines proposed by Magnanini & Tolio [34]. The behavior of each stage in isolation (without accounting for joint system dynamics) is modeled by a discrete-state continuous-time Markov Chain. When the unit process is considered in isolation its behavior is not impeded by other resources in the system, and it is characterized by two states: a productive state P, and a down state D. When it is in the productive state P, the unit process manufactures one part every cycle time CT^{k}. When it is in the down state D, some disruptive event occurred, as a failure or a breakage. In this state, the unit process does not manufacture any part. Since the transitions between states occur stochastically, a Markov Chain is adopted, and its transition rate matrix Q^{k} can be defined according to the unit-process parameters, as per Eq. 3,

$$Q^{\mathrm{k}} = \begin{bmatrix} -f^{\mathrm{k}} & f^{\mathrm{k}} \\ r^{\mathrm{k}} & -r^{\mathrm{k}} \end{bmatrix} \quad , \quad \forall \mathrm{k} = \mathrm{AM}, \mathrm{SM} \tag{3}$$

where

- r^{k} (in h^{-1}) is the average repair rate, equal to $1/MTTR^{\mathrm{k}}$;
- f^{k} (in h^{-1}) is the average failure rate, equal to $1/MTTF^{\mathrm{k}}$, for either $k = \mathrm{AM}$ or $k = \mathrm{SM}$.

MTTR and *MTTF* are assumed to be the mean of the exponential distribution characterizing the time to repair and the time to failure, respectively. In this context, the efficiency in isolation is defined as the expected percentage of time during which the single unit process remains productive, if not impeded by other resources in the system. This is formalized in Eq. 4:

$$e^{\mathrm{k}} = \frac{r^{\mathrm{k}}}{r^{\mathrm{k}} + f^{\mathrm{k}}} \quad , \quad \forall \mathrm{k} = \mathrm{AM}, \mathrm{SM} \tag{4}$$

If a general distribution rather than an exponential distribution is considered, empirical distributions such as Phase Types can be modeled according to literature [36]. Grounding on the single unit-process characterization and inter-operational buffer capacity, equal to N, the system state-space can be defined by the triplet $(n,\ S^{\mathrm{AM}},\ S^{\mathrm{SM}})$, where n is a continuous variable representing the buffer level (ranging from 0 to N), according to the Kronecker product (i.e., the combination of all possible resource states). Specific states emerge from the system-level representation as a consequence of the resource interaction:

- Blocking state: $B = (N, P, D)$, in which even if the upstream unit process can be productive, no part is processed;
- Starvation state: $S = (0, D, P)$, in which even if the downstream unit process can be productive, no part is processed.

The performance evaluation model allows estimating the steady-state probabilities of the unit-process states at the system level. Following the solution method proposed in Tolio & Ratti [47] and Magnanini & Tolio [34] for a discrete two-stage manufacturing line with Markovian behavior, the system-level Markov Chain is solved by means of a linear system of partial differential stochastic equations and the steady-state probabilities can be found. In particular, π_i^{k} (-) is the steady-state probability of the k-th unit process (i.e., for either $k = \mathrm{AM}$ or $k = \mathrm{SM}$) being operational ($i = \mathrm{P}$), or blocked ($i = \mathrm{B}$), or starved ($i = \mathrm{S}$), or failed ($i = \mathrm{D}$). By definition, the relations in Eq. 5 and Eq. 6 hold for AM and SM, respectively:

$$\pi_{\mathrm{P}}^{\mathrm{AM}} + \pi_{\mathrm{D}}^{\mathrm{AM}} + \pi_{\mathrm{B}}^{\mathrm{AM}} = 1 \tag{5}$$

$$\pi_{\mathrm{P}}^{\mathrm{SM}} + \pi_{\mathrm{D}}^{\mathrm{SM}} + \pi_{\mathrm{S}}^{\mathrm{SM}} = 1 \tag{6}$$

The analytical method used in this work is equivalent to a DES model where the steady-state probabilities are obtained as percentages of the time spent by the single unit process in each state, with respect to the total simulation time. Finally, the system throughput TH (in part/h) can be computed as per Eq. 7:

$$TH = \frac{1}{CT^{\mathrm{k}}} \cdot \pi_{\mathrm{P}}^{\mathrm{k}} \quad , \quad \forall \mathrm{k} = \mathrm{AM}, \mathrm{SM} \tag{7}$$

2.3. Environmental impact assessment

Once the outputs of the characterization of each unit process (Section 2.1) and the system performance evaluation (Section 2.2) are both available, the electrical energy consumption for producing a number of parts in a given time interval (which is labeled as $E_{\Delta \mathrm{t}}^{\mathrm{k}}$ and measured in kWh) can be computed according to Eq. 8, for any k-th unit process and by accounting for the different i-th operational modes,

$$E_{\Delta \mathrm{t}}^{\mathrm{k}} = \sum_i \overline{P_{\mathrm{i}}^{\mathrm{k}}} \cdot \pi_{\mathrm{i}}^{\mathrm{k}} \cdot \Delta \mathrm{t} \quad , \quad \forall \mathrm{k} = \mathrm{AM}, \mathrm{SM} \tag{8}$$

where

- $\overline{P_{\mathrm{i}}^{\mathrm{k}}}$ (kW) is the average power demand of the manufacturing equipment when operational ($i = \mathrm{P}$), or blocked ($i = \mathrm{B}$), or starved ($i = \mathrm{S}$), or failed ($i = \mathrm{D}$), for either $k = \mathrm{AM}$ or $k = \mathrm{SM}$;
- $\Delta \mathrm{t}$ (h) is the considered time interval (e.g., a work shift).

Eq. 8 has general validity. In this study it is assumed that when a machine is idling due to blocking, starvation or intervention, a constant power demand is required, equal to $\overline{P_{\mathrm{idle}}^{\mathrm{k}}}$. Therefore, the AM and SM unit processes can be either productive or idling. Therefore, the total electrical energy consumption of the hybrid additive-subtractive manufacturing approach, $E_{\Delta \mathrm{t}}$ (in kWh), can be written according to Eq. 9,

$$E_{\Delta \mathrm{t}} = E_{\Delta \mathrm{t}}^{\mathrm{AM}} + E_{\Delta \mathrm{t}}^{\mathrm{SM}} = \left[\left(\overline{P_{\mathrm{P}}^{\mathrm{AM}}} \cdot \pi_{\mathrm{P}}^{\mathrm{AM}} + \overline{P_{\mathrm{idle}}^{\mathrm{AM}}} \cdot \pi_{\mathrm{idle}}^{\mathrm{AM}} \right) + \left(\overline{P_{\mathrm{P}}^{\mathrm{SM}}} \cdot \pi_{\mathrm{P}}^{\mathrm{SM}} + \overline{P_{\mathrm{idle}}^{\mathrm{SM}}} \cdot \pi_{\mathrm{idle}}^{\mathrm{SM}} \right) \right] \cdot \Delta \mathrm{t} \tag{9}$$

where, for consistency with Eq. 5 and Eq. 6:

- $\pi_{idle}^{AM} = \pi_{D}^{AM} + \pi_{B}^{AM}$, for k = AM;
- $\pi_{idle}^{SM} = \pi_{D}^{SM} + \pi_{S}^{SM}$, for k = SM.

To quantify the selected environmental impact metrics, the contributions of all the j-th consumables (such as the shielding gas for WAAM, or the cutting tool(s) and the lubricant(s) for CNC machining) have to be added. Therefore, the cumulative (primary) energy demand for the gate-to-gate system boundary, $CED_{\Delta t}$ (in MJ), required in the selected time interval Δt, can be quantified according to Eq. 10:

$$CED_{\Delta t} = \frac{3.6}{\eta} \cdot E_{\Delta t} + \sum_{j,k} E_j \cdot \dot{q}_j^k \cdot \overbrace{\pi_P^k \cdot \Delta t}^{t_P^k} \tag{10}$$

where

- the factor 3.6 converts kWh to MJ;
- η (-) is the primary-to-secondary energy conversion coefficient, which accounts for the energy losses occurring during the production of electricity from primary energy sources;
- E_j (MJ/kg or MJ/m^3) is the primary energy embodied in a unit mass or volume of the j-th consumable;
- $\dot{q}_j^k$ (to be measured in kg/h or in m^3/h) is the consumption rate of each j-th consumable, for either k = AM or k = SM.

Eq. 10 implies that the consumption of consumable resources is addressed only to the unit-process operational time (t_P^k). This hypothesis is consistent with the hybrid process that has been considered, as it is realistic to assume that no shielding gas, tools or lubricants are consumed when the machines are blocked, starved or stopped for maintenance interventions (when the unit processes are not producing parts). In addition, the ancillary material inputs that amortize over the production of multiple parts (such as maintenance kits and materials) and the system components that amortize over their respective lifespans can be assumed as negligible on a per-part basis assessment.

Then, being the throughput of the system available (Eq. 7), the number of parts produced during the selected time interval Δt can be obtained as $TH \cdot \Delta t$. Therefore, to calculate the CED to be allocated to each single produced component (CED_{part}, in MJ/part), Eq. 11 can be applied,

$$\begin{aligned} CED_{part} &= \frac{CED_{\Delta t}}{TH \cdot \Delta t} \\ &= \frac{3.6}{\eta} \cdot \frac{\left[\left(\overline{P_P^{AM}} \cdot \pi_P^{AM} + \overline{P_{idle}^{AM}} \cdot \pi_{idle}^{AM} \right) + \left(\overline{P_P^{SM}} \cdot \pi_P^{SM} + \overline{P_{idle}^{SM}} \cdot \pi_{idle}^{SM} \right) \right]}{TH} \\ &\quad + \frac{\sum_{j,k} E_j \cdot \dot{q}_j^k \cdot \pi_P^k}{TH} \end{aligned} \tag{11}$$

where the two separate contributions due to electrical energy consumption and consumable resources can be identified on a per-part basis. It should be emphasized that, in this way, the energy consumed when idling (i.e., when the unit process is either blocked, or starved, or failed) is divided equally over the parts produced in the considered time interval. Please note that similar approach was used, at single unit-process level, by Frigerio & Matta [17]. The carbon dioxide emissions associated with the production of a single part, $CO_{2\ part}$ (in kgCO_2/part), can be similarly determined using Eq. 12,

$$\begin{aligned} CO_{2\ part} &= CES \cdot \frac{\left[\left(\overline{P_P^{AM}} \cdot \pi_P^{AM} + \overline{P_{idle}^{AM}} \cdot \pi_{idle}^{AM} \right) + \left(\overline{P_P^{SM}} \cdot \pi_P^{SM} + \overline{P_{idle}^{SM}} \cdot \pi_{idle}^{SM} \right) \right]}{TH} \\ &\quad + \frac{\sum_{j,k} CO_{2j} \cdot \dot{q}_j^k \cdot \pi_P^k}{TH} \end{aligned} \tag{12}$$

where

- CES (kgCO_2/kWh) is the carbon emission signature of the electric grid, as defined by Jeswiet & Kara [24];
- CO_{2j} (kgCO_2/kg or kgCO_2/m^3) is the carbon footprint of the j-th consumable.

It is worth noting that, when referring to consumables, their contribution becomes a fixed share in the assessment of the environmental impact per produced part, as demonstrated in Eq. 13, as they do not depend on the system configuration, i.e., the interaction dynamics of the two processes:

$$CED_{consumables} = \frac{\sum_{j,k} E_j \cdot \dot{q}_j^k \cdot \pi_P^k}{TH} = \sum_{j,k} E_j \cdot \dot{q}_j^k \cdot CT^k. \tag{13}$$

3. Case study

A case study to clarify the implementation of the methodology is presented in this section. A manufacturing line made of two separate machines for additive manufacturing and finish machining is considered. In particular, additive manufacturing is carried out using a WAAM machine based on the Cold Metal Transfer (CMT) technology, and subtractive manufacturing is performed by means of a CNC milling machine. A mock-up of a propeller is considered as the part to be produced (Fig. 3). The WAAM process required 1.32 kg of feedstock metal wire, and the as-built part weighed 1.30 kg. Material loss was due to welding spatter and some cutting of the welding wire [6]. The resultant material utilization efficiency of the WAAM process was approximately 98.5 %. The mass of the finish-machined component was 0.72 kg, which was achieved by removing 0.58 kg of chips from the near-net-shape WAAM-ed part by contour milling. For the purposes of the analysis, one configuration is considered for the WAAM unit process, while three scenarios for machining (with one configuration either slower, approximately equal, and faster than WAAM) are envisaged to foster the discussion of the results. The data collection is described in detail in Section 3.1 and Section 3.2 for the WAAM and the machining unit process, respectively [15]. Unless otherwise stated, electric energy consumption is reported in kWh, while energy values in MJ refer to the primary energy level [18]. A primary-to-secondary energy conversion efficiency of 0.38 was assumed [3], while the greenhouse gas emission intensity of electricity generation was set at 0.21 kgCO_2/kWh (i.e., the 2023-average value for the EU27, according to the indicators of the European Environment Agency [14]).

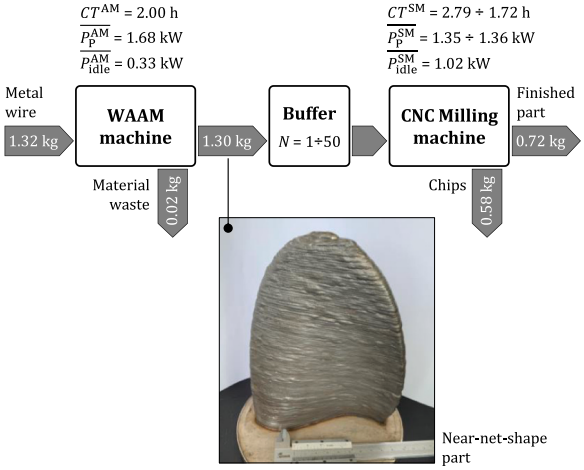

Fig. 3. Case study and main input data.

3.1. Data inventory for the WAAM unit process

The data for the WAAM unit process refer to a custom-built machine based on Cold Metal Transfer (CMT) as the deposition process, using a Fronius CMT system equipped with a TPS 400i generator [39]. The translation of the deposition head (along the X, Y and Z axes) and the rotation of the baseplate (around the C axis) are controlled by a 4-axis Siemens Sinumerik 840 CNC system. The machine is housed in a safety cell equipped with an industrial fume extraction system (active only when the machine is operational), whose power demand has been taken into account in the calculation of the total energy consumption of the AM system. A Ø 1.2-mm AWS ER 308 L Si steel wire was used as the feedstock material. The wire feed speed (*WFS*) and the travel speed (*TS*) were set to 4 m/min and 0.5 m/min, respectively, while the deposition power was automatically adjusted on the basis of the CMT 3556 Universal synergic curve. The deposition path, having 67 superimposed layers, was designed using a dedicated CAM software. An overlap factor of 0.74 *w* (where *w* is the width of the bead) was chosen in the case of side-by-side deposited beads, according to Ding et al. [11]. The inter-layer cooling time was obtained by setting the interpass temperature to 400°C, which was controlled by an infrared pyrometer. An Ar + 2.5 % CO_2 shielding gas was supplied to the deposition area to prevent material oxidation. Three-phase Fluke 430 Series II analysers were used to characterize the electric energy consumption of the whole unit process, which is reported in Table 1.

The average power demand of the AM system when productive, $\overline{P_P^{AM}}$, was computed as the ratio between the values measured in field of E_{CT}^{AM} and CT^{AM}, according to Eq. 1. Nevertheless, the electric energy consumption for manufacturing a single part, E_{CT}^{AM}, could also be obtained as per Eq. 2, when the values of $\overline{P_{on}^{AM}}$, $\overline{P_{off}^{AM}}$ and $\overline{P_{stb}^{AM}}$ (equal to 4.07, 0.87 and 0.33 kW, respectively) are available from a preliminary characterization of the AM system. The average deposition rate (i.e., the ratio between the amount of deposited material and the arc-on time) was found to be 2.5 kg/h, and the specific energy consumption in this phase was 1.66 kWh/kg of deposited material. These results are in agreement with other available literature sources [9], even if different setups are used [38]. The Ar + 2.5 % CO_2 shielding gas was the only consumable resource required for the WAAM unit process (when depositing), with a consumption rate ($\dot{q}_{gas}^{AM}$) of approximately 1.5 kg/h. The gas was not recaptured during the process. The embodied energy (E_{gas}) and the carbon footprint ($CO_{2\ gas}$) of the shielding gas were assumed as 8 MJ/kg and 0.2 kgCO_2/kg, respectively (adapted from [21]). Therefore, the resultant impacts were estimated as 6.4 MJ and 0.17 kgCO_2 per additively manufactured part. The *MTTF* and *MTTR* for WAAM machines can vary depending on the specific equipment/process being used, the skills of the operators and maintenance personnel, the complexity of the problem and the availability of spare parts. In general, simple issues such as wire feed problems or torch malfunctions can often be resolved within a limited time. More complex issues, such as problems with the control system or power supply, may require more time and specialized expertise to resolve. To the sake of exemplification, the efficiency of the WAAM system in isolation e^{AM} was varied in this research from 80 % (worst case) to 90 % (best case). In the absence of specific data for the WAAM process in the current literature, these values have been selected based on standard industrial references, as reported by Alaouchiche et al. [1].

Table 1
Energy consumption and power demand for the WAAM unit process.

Parameter	Unit	Value
Setup time, t_{set}^{AM}	h	0.16
Active material deposition (arc-on) time, t_{on}	h	0.53
Dwell (arc-off) time for inter-layer cooling, t_{off}	h	1.31
Cycle time for single-part manufacturing, CT^{AM}	h	2.00
Electric energy consumption for single part manufacturing, E_{CT}^{AM}	kWh	3.35
Average power demand of the AM system when productive, $\overline{P_P^{AM}}$	kW	1.68
Average power demand of the AM system when idling, $\overline{P_{idle}^{AM}}$	kW	0.33

3.2. Data inventory for the machining unit process

The characterization of the machining unit process can be carried out experimentally, by replicating the procedure outlined in the previous Section 3.1 for the WAAM unit process. Alternatively, theoretical and empirical models can also be exploited to collect data, and can be useful for the preliminary evaluation of different scenarios, as illustrated in this section. During the machining process, the Material Removal Rate (*MRR*) has been found to be the decisive factor in determining the energy consumption for a given machine tool, and an inverse relationship between the Specific Energy Consumption (*SEC*) and the *MRR* can be established [30]. In this case study, the unit-process energy consumption was computed by assuming a *SEC* (kJ/cm^3) = 2.830 + 1.344 / *MRR* (cm^3/s) model, and a fixed power consumption of 1.02 kW when the machine is on standby [25]. This modeling approach, as opposed to using average processing energy values from LCA software databases, allows energy requirements to be quantified as the chosen process configuration changes. The milling parameters were selected based on the recommendations provided by the tool suppliers. Three levels of *MRR* were identified for both semi-finishing and finishing (the latter limited to 12 % of the mass of chips removed), within a reasonable range of process parameters. It is worth noting that the *MRR* values reported in Table 2 are comparable to those employed by Campatelli et al. [7] for (semi-)finishing WAAM-ed steel components, and lower than those reported by Priarone et al. [40], where bigger tools and higher removal rates were used due to the larger size of the components. The Specific Energy Consumption (*SEC*) only considers the energy required during the processing period, while the energy consumed during machine startup, standby, clamping and positioning periods is disregarded [25]. Therefore, to ensure that the assessment of energy consumption per part is consistent with the assumptions made for the WAAM unit process, a

Table 2
Energy consumption and power demand for the machining unit process. Three scenarios are considered: a slower one (#1), one approximately equal (#2), and a faster one (#3) than the WAAM process.

Parameter	Unit	Scenario #1	Scenario #2	Scenario #3
Material removal rate for the semi-finishing operation, MRR_{sf}	kg/h	0.55	0.69	0.83
Material removal rate for the finishing operation, MRR_f	kg/h	0.04	0.06	0.07
Standby time, t_{stb}^{SM}	h	0.12	0.12	0.12
Milling time for the semi-finishing operation, t_{sf}	h	0.93	0.74	0.61
Milling time for the finishing operation, t_f	h	1.74	1.16	0.99
Cycle time for single-part manufacturing, CT^{SM}	h	2.79	2.02	1.72
Electric energy consumption for standby, E_{stb}^{SM}	kWh	0.12	0.12	0.12
Electric energy consumption for semi-finishing, E_{sf}^{SM}	kWh	1.30	1.05	0.88
Electric energy consumption for finishing, E_f^{SM}	kWh	2.35	1.57	1.34
Electric energy consumption for single part manufacturing, E_{CT}^{SM}	kWh	3.77	2.74	2.34
Average power demand of the SM system when productive, $\overline{P_P^{SM}}$	kW	1.35	1.36	1.36
Average power demand of the SM system when idling, $\overline{P_{idle}^{SM}}$	kW	1.02	1.02	1.02

separate standby energy demand was included in the calculation. The data presented in Table 2 shows how, for the same amount of material removed, the energy consumption decreases as the *MRR* increases, as expected from the application of the *SEC* model. The average power demand for processing a part remains largely unchanged across the different scenarios, based on the assumptions made in this study. Nonetheless, the limited impact of the cutting process on the overall energy consumption of the machine tool and its equipment has already been acknowledged by Behrendt et al. [5].

Dry cutting conditions were preferred due to their cost and environmental benefits [48]. Therefore, cutting tools were considered as the only consumable resource in the machining unit process. Dahmus & Gutowski [10] pointed out that the direct environmental impact of tools is generally limited when assessed on a per-part basis. For this specific case study, the following assumptions were made: (*i*) the use of a ball nose endmill with two replaceable carbide inserts, each with two cutting edges, for both semi-finishing and finishing; (*ii*) the precautionary repositioning of the indexable inserts after each machined part, representing a worst-case scenario; (*iii*) an embodied impact of 2.7 MJ and 0.22 $kgCO_2$ per cutting edge, according to the cutting tool data reported in Priarone et al. [41] for coated carbide inserts weighing approximately 10 g. Under these assumptions, a contribution to *CED* and total carbon dioxide emissions of 5.4 MJ and 0.44 $kgCO_2$ per manufactured part was added due to the cutting tool consumption. Lastly, modern machining centers are designed for high reliability and can run for long periods of time. However, tool breakage, problems with the power supply, spindle, coolant or control systems and various other factors can lead to unplanned downtime. In the absence of precise values, the efficiency of the SM system in isolation (e^{SM}) has been estimated between 80 % and 90 %, in order to maintain consistency with the assumptions made for the AM unit process. This range aligns with findings from existing studies on energy control in machining systems, such as Wójcicki at al. [49].

4. Results and discussion

This section presents the numerical results of the evaluated scenarios, focusing on the three targeted performance indicators: the cumulative energy demand per part (CED_{part} in MJ/part, computed according to Eq. 11), the equivalent CO_2 emissions per part ($CO_{2\ part}$ in $kgCO_2$/part, as per Eq. 12), and the production throughput (*TH* in part/hour, as defined in Eq. 7). For each scenario, the effect of the intermediate buffer capacity (*N*) on these indicators was evaluated, with extreme configurations represented by buffer sizes of $N = 1$ and $N = 50$ parts. Fig. 4 highlights the variations in CED_{part} results across the different scenarios (see Table 2). The energy demand per part is influenced by system-level interactions. Scenario 1, exhibiting significant imbalance in cycle times between the AM and SM stages, yields suboptimal energy demand performance relative to the configuration where resources are more balanced (Scenario 2). Although Scenario 3 is imbalanced (like Scenario 1), it exhibits better energy performance since its slowest stage is still faster than the slowest stage in Scenario 1. As a result, the maximum achievable throughput in Scenario 3 is higher than that of Scenario 1, as discussed in the following.

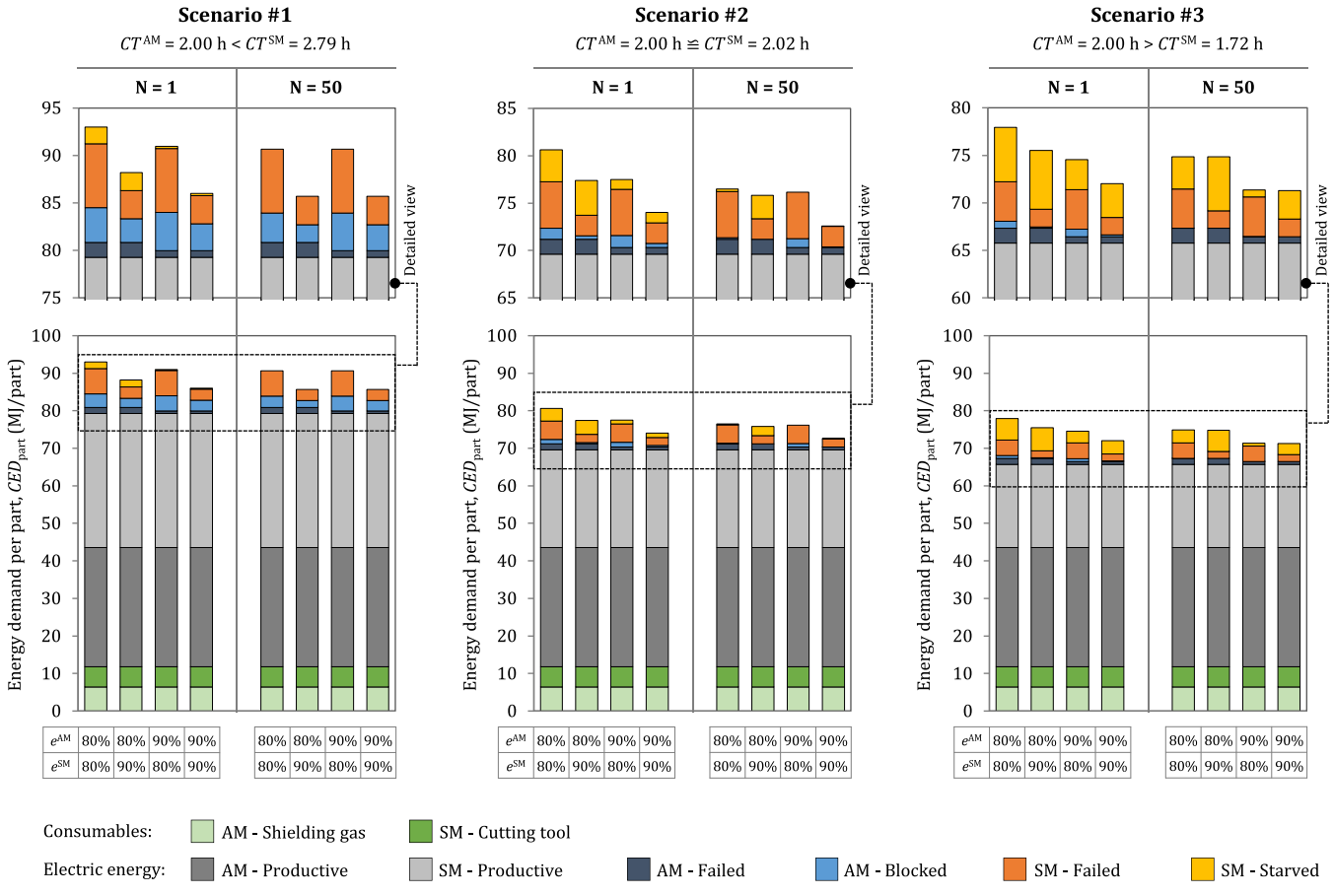

Fig. 4. Contributions to the cumulative energy demand per part (CED_{part}) as a function of buffer size ($N = 1$ or $N = 50$), for the three considered scenarios and different combinations of unit-process efficiencies (e^{AM} and e^{SM}).

The energy demand per part due to productive states does not change across the different configuration scenarios. The results presented in Fig. 4 also allow highlighting the impact of assuming a purely deterministic process representation on the quantification of cumulative energy demand (CED_{part}). When the effects of failure, blocking, and starvation are neglected (assuming decoupled stages with infinite buffer capacity and disregarding disruptive micro-stoppages), the CED_{part} amounts to 79, 70, and 66 MJ/part for Scenarios 1, 2, and 3, respectively. This represents a deviation ranging from 5 % to 15 % compared with the values obtained using the proposed stochastic model. By integrating system-level dynamics into the environmental assessment, the interdependencies among unit processes are explicitly accounted for, resulting in more representative sustainability indicators at the system level. The observed differences primarily stem from energy consumption during non-productive states. These variations can be explained by the performance evaluation results detailed in Table 3. Specifically, higher variability in stoppages (indicated by lower efficiency in isolation) and cycle time imbalance increase the occurrence of blocking and starvation phenomena, thereby raising the likelihood of the system entering idle states. As a consequence, energy demand per part increases due to prolonged periods in non-productive but still power-demanding states (on average, 29 % blocking probability in Scenario 1 and 16 % starvation probability in Scenario 3).

Increasing the buffer capacity contributes to the reduction of the energy demand per part. Specifically, comparing the performance of each scenario under the two buffer configurations ($N = 1$ and $N = 50$), the latter consistently yields lower energy demand. This is due to the enhanced decoupling between the process stages, which reduces the probability of blocking and starvation events. A more detailed analysis in Fig. 5 highlights the influence of buffer configuration on CED_{part}. Once a certain degree of decoupling is achieved through buffer expansion, the energy demand reaches a plateau, becoming primarily dependent on the characteristics of the system bottleneck. For example, in Scenario 1, the subtractive manufacturing (SM) stage acts as the bottleneck, limiting productivity according to Eq. 14,

$$TH_{\text{limit}} = \frac{1}{CT^{\text{SM}}} \cdot e^{\text{SM}} \tag{14}$$

yielding TH_{limit} for $e^{\text{SM}} = 80$ % of 0.29 part/hour and TH_{limit} for e^{SM}

Table 3
Steady-state probabilities of the k-th unit process (i.e., for k = AM or k = SM) being productive, blocked, starved, or failed.

Scenario	e^{AM} (%)	e^{SM} (%)	N (parts)	$\pi_{\text{P}}^{\text{AM}}$ (%)	$\pi_{\text{idle}}^{\text{AM}}$ (%)		$\pi_{\text{P}}^{\text{SM}}$ (%)	$\pi_{\text{idle}}^{\text{SM}}$ (%)	
					$\pi_{\text{D}}^{\text{AM}}$ (%)	$\pi_{\text{B}}^{\text{AM}}$ (%)		$\pi_{\text{D}}^{\text{SM}}$ (%)	$\pi_{\text{S}}^{\text{SM}}$ (%)
#1	80	80	1	54.5	13.6	31.9	76.0	19.0	5.0
			5	56.8	14.2	29.0	79.2	19.8	1.0
			10	57.3	14.3	28.4	79.9	20.0	0.1
			20	57.3	14.3	28.3	80.0	20.0	0.0
		90	1	60.7	15.2	24.2	84.6	9.4	6.0
			5	63.6	15.9	20.5	88.7	9.8	1.4
			10	64.3	16.1	19.6	89.8	10.0	0.3
			20	64.5	16.1	19.3	90.0	10.0	0.0
	90	80	1	57.0	6.3	36.7	79.5	19.9	0.6
			5	57.3	6.4	36.3	80.0	20.0	0.0
			10	57.3	6.4	36.3	80.0	20.0	0.0
			20	57.3	6.4	36.3	80.0	20.0	0.0
		90	1	64.0	7.1	28.9	89.3	9.9	0.8
			5	64.5	7.2	28.3	90.0	10.0	0.0
			10	64.5	7.2	28.3	90.0	10.0	0.0
			20	64.5	7.2	28.3	90.0	10.0	0.0
#2	80	80	1	69.5	17.4	13.1	70.2	17.6	12.2
			5	73.3	18.3	8.3	74.1	18.5	7.4
			10	75.3	18.8	5.8	76.1	19.0	4.9
			20	77.0	19.2	3.8	77.8	19.4	2.8
		90	1	76.3	19.1	4.7	77.0	8.5	14.4
			5	78.9	19.7	1.4	79.7	8.8	11.5
			10	79.7	19.9	0.4	80.5	8.9	10.6
			20	80.0	20.0	0.0	80.8	9.0	10.3
	90	80	1	76.1	8.4	15.5	76.8	19.2	4.0
			5	78.4	8.7	12.9	79.2	19.8	1.0
			10	79.0	8.8	12.2	79.8	20.0	0.2
			20	79.2	8.8	12.0	80.0	20.0	0.0
		90	1	84.7	9.4	5.9	85.6	9.5	4.9
			5	87.2	9.7	3.2	88.0	9.8	2.2
			10	88.1	9.8	2.1	89.0	9.9	1.2
			20	88.7	9.8	1.5	89.6	9.9	0.5
#3	80	80	1	73.0	18.2	8.8	62.8	15.7	21.6
			5	76.9	19.2	3.9	66.1	16.5	17.3
			10	78.7	19.7	1.6	67.7	16.9	15.4
			20	79.7	19.9	0.3	68.6	17.1	14.3
		90	1	78.4	19.6	2.0	67.4	7.5	25.1
			5	79.8	20.0	0.2	68.7	7.6	23.7
			10	80.0	20.0	0.0	68.8	7.6	23.6
			20	80.0	20.0	0.0	68.8	7.6	23.6
	90	80	1	80.7	9.0	10.3	69.4	17.4	13.2
			5	85.1	9.5	5.4	73.2	18.3	8.5
			10	87.2	9.7	3.1	75.0	18.8	6.2
			20	88.8	9.9	1.4	76.3	19.1	4.6
		90	1	87.8	9.7	2.4	75.5	8.4	16.1
			5	89.7	10.0	0.3	77.2	8.6	14.3
			10	90.0	10.0	0.0	77.4	8.6	14.0
			20	90.0	10.0	0.0	77.4	8.6	14.0

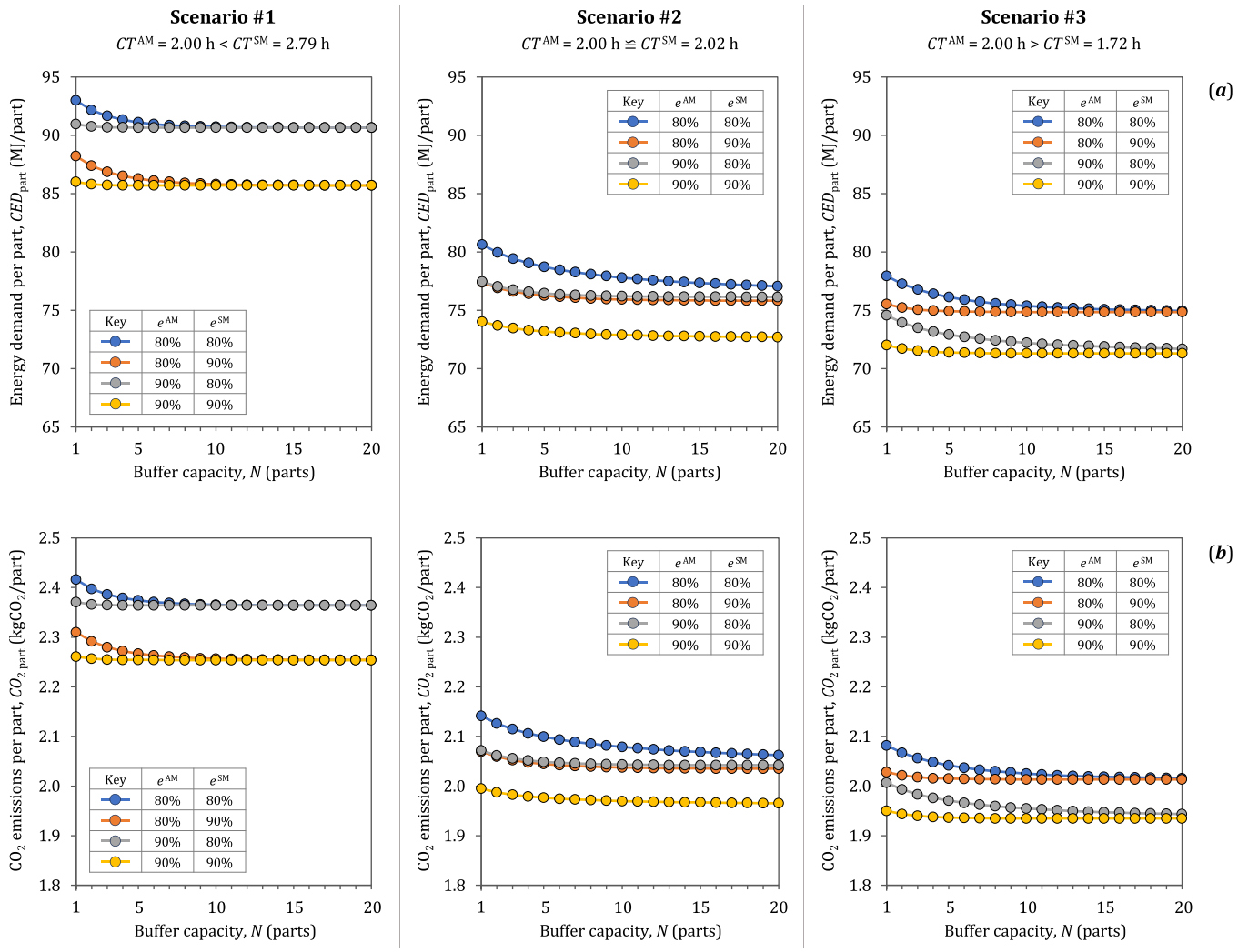

Fig. 5. Results of cumulative energy demand (*a*) and equivalent carbon dioxide emissions (*b*) per part as a function of buffer capacity, for the three considered scenarios and different combinations of unit-process efficiencies (e^{AM} and e^{SM}).

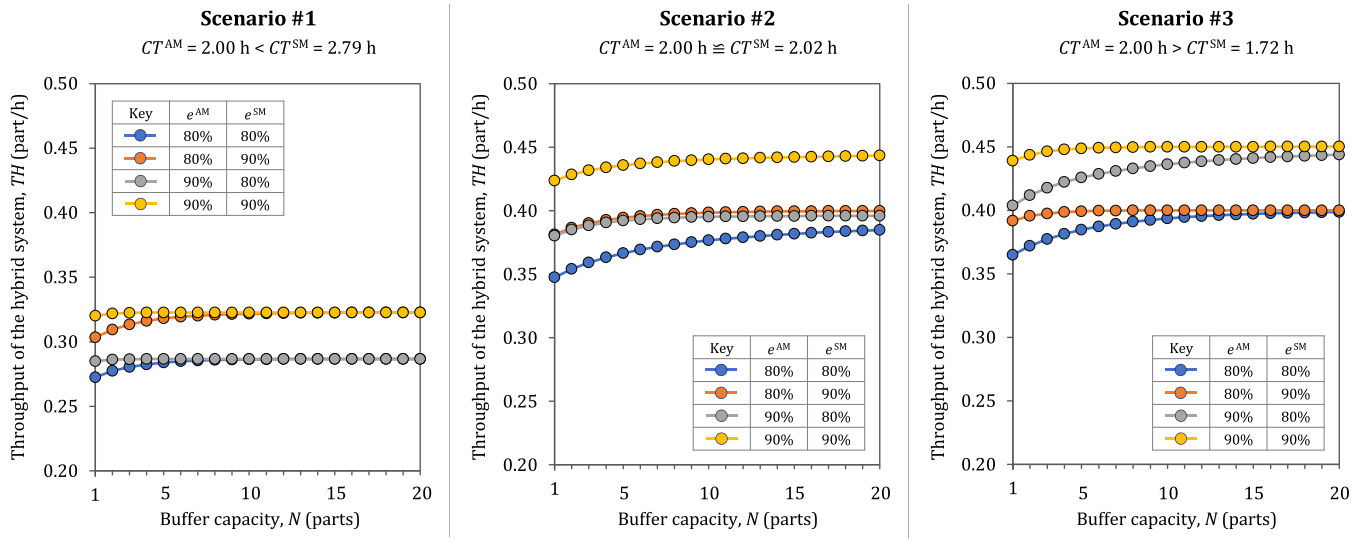

Fig. 6. Results of throughput of the hybrid WAAM-subtractive system as a function of buffer capacity, for the three considered scenarios and different combinations of unit-process efficiencies (e^{AM} and e^{SM}).

= 90 % of 0.32 part/hour. These limiting values are reflected in Fig. 6, where throughput saturates regardless of buffer size, constrained by the maximum capacity of the bottleneck. As a direct consequence, lower bounds can also be defined for both energy demand per part and CO_2 emissions per part, determined by the intrinsic characteristics of the process stages. On the other hand, larger buffer capacities imply increased work-in-progress (*WIP*) and lead time. Therefore, the final system configuration should be selected by balancing conflicting objectives, according to specific performance priorities and the adopted cost model.

Overall, from an environmental impact perspective, Fig. 7 summarizes the trade-offs between system throughput and cumulative energy demand (Fig. 7*a*) or equivalent CO_2 emissions (Fig. 7*b*) per part. Each data point represents a specific buffer configuration within a scenario and a given combination of unit-process efficiencies (e^{AM} and e^{SM}). The trajectories connecting points within the same configuration confirm the effect of increasing buffer capacity (from left to right in each cluster): larger buffers mitigate blocking and starvation phenomena, as previously discussed, allowing the system throughput to approach its theoretical upper bound (as determined by the bottleneck stage), while reducing idle-time energy consumption. This results in lower specific energy demand and, consequently, reduced CO_2 emissions per part, as increasing buffer capacity reduces the effect of stochastic variability.

Notably, the shape of the curves exhibits a decreasing trend with increasing the system throughput, a behavior consistent with well-established evidence for single-unit processes, as production systems typically show lower energy intensities at higher output rates [22]. However, while the available models are generally limited to individual unit processes [25], the results presented here refer to system-level indicators, accounting for dynamic interactions between sequential stages, including blocking, starvation, and inter-stage decoupling. This underscores how energy and emission outcomes could be influenced not only by the efficiency of individual processes, but also by the system architecture and its control logic.

Furthermore, the approach adopted in this work, which serves as a tool to support strategic decision-making during process planning, advances conventional sustainability assessments typically found in the literature, which often rely on linear and additive estimations of environmental and economic impacts [40]. In those analyses, the total footprint is approximated by summing the independent contributions of the additive and subtractive stages in isolation, neglecting the effects of interdependencies, buffer sizing, and system-level inefficiencies. As a result, such methods may underestimate the actual energy consumption and carbon footprint of hybrid manufacturing systems where different unit processes are interconnected.

4.1. Sensitivity analysis

When applying the model to the case study, some parameters were sourced from recent literature and/or established scientific databases, and cross-checked whenever possible. Although the results are necessarily specific to the chosen case and dataset, the main objective of the study was to demonstrate the applicability of the proposed model. Using secondary data is a common practice when primary measurements are unavailable or when exploring alternative scenarios, as in this case, though it may affect the robustness of quantitative estimates. The sensitivity of throughput (*TH*) and cumulative energy demand per part (CED_{part}) was analyzed with respect to *MTTF*, considering alternative levels of efficiency in isolation for each stage. The finite buffer capacity was set to $N = 5$, and parameters were selected within reasonable ranges. Specifically, the $MTTF^k$ for each *k*-th stage was varied from an average failure every 2 parts to a maximum of every 15 parts (relative to the cycle time), while maintaining the overall efficiency of the stage constant. Consequently, the $MTTR^k$ was varied as a function of both efficiency and $MTTF^k$. The results are presented in Fig. 8 and Fig. 9 as iso-performance curves, with a consistent color scale applied across all cases within the same scenario. In each graph, a red dot highlights the performance metrics corresponding to the *MTTF* values used in the case study to discuss the results presented in the previous section. Productivity and environmental metrics are primarily sensitive to the cycle time of each stage, rather than the assumed *MTTF/MTTR* parameters. For instance, throughput in Scenario 1 (the worst case) ranges from 0.28 to 0.32 part/h, whereas in Scenarios 2 and 3 it ranges from 0.36 to 0.45 part/h. These intervals do not overlap, and a similar pattern is observed for CED_{part}: Scenario 1 ranges from 85 to 91 MJ/part, while Scenarios 2 and 3 range from 71 to 79 MJ/part. Within each scenario, differences due to stage efficiency in isolation can be appreciated, consistent with the observations reported for Fig. 5 and the discussion in Section 3.

The sensitivity analysis also highlights the impact of system dynamics. For instance, Scenario 1 exhibits iso-performance curves with a generally vertical pattern, whereas Scenario 3 shows predominantly horizontal curves. In Scenario 1, the subtractive stage (SM) is the bottleneck in terms of cycle time. Consequently, any marginal reduction in the variability of the *MTTF* of the additive stage (AM), even at the same efficiency in isolation, leads to a slight improvement in environmental performance, as productivity increases and the time spent by the

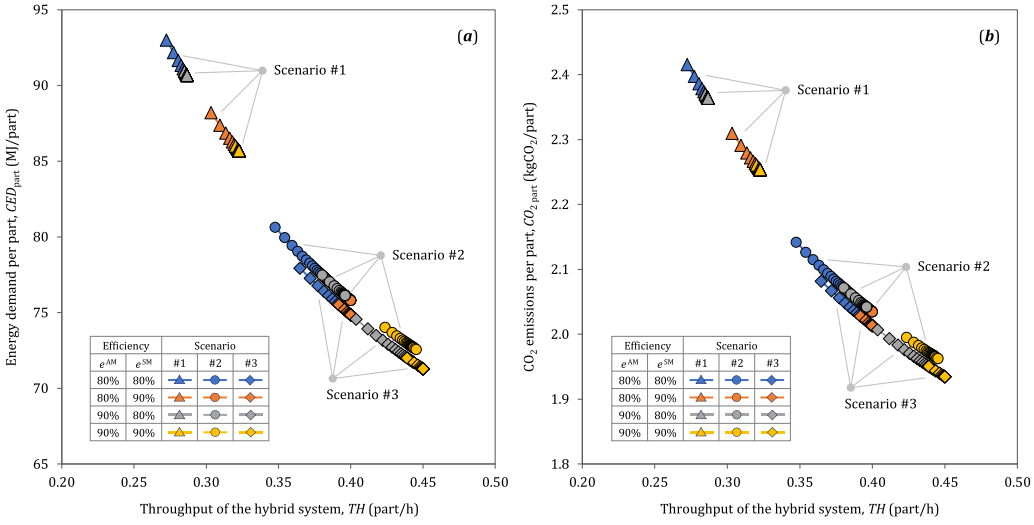

Fig. 7. Results of cumulative energy demand (*a*) and CO_2 emissions (*b*) per part as a function of the system throughput, for the three considered scenarios and different combinations of unit-process efficiencies (e^{AM} and e^{SM}).

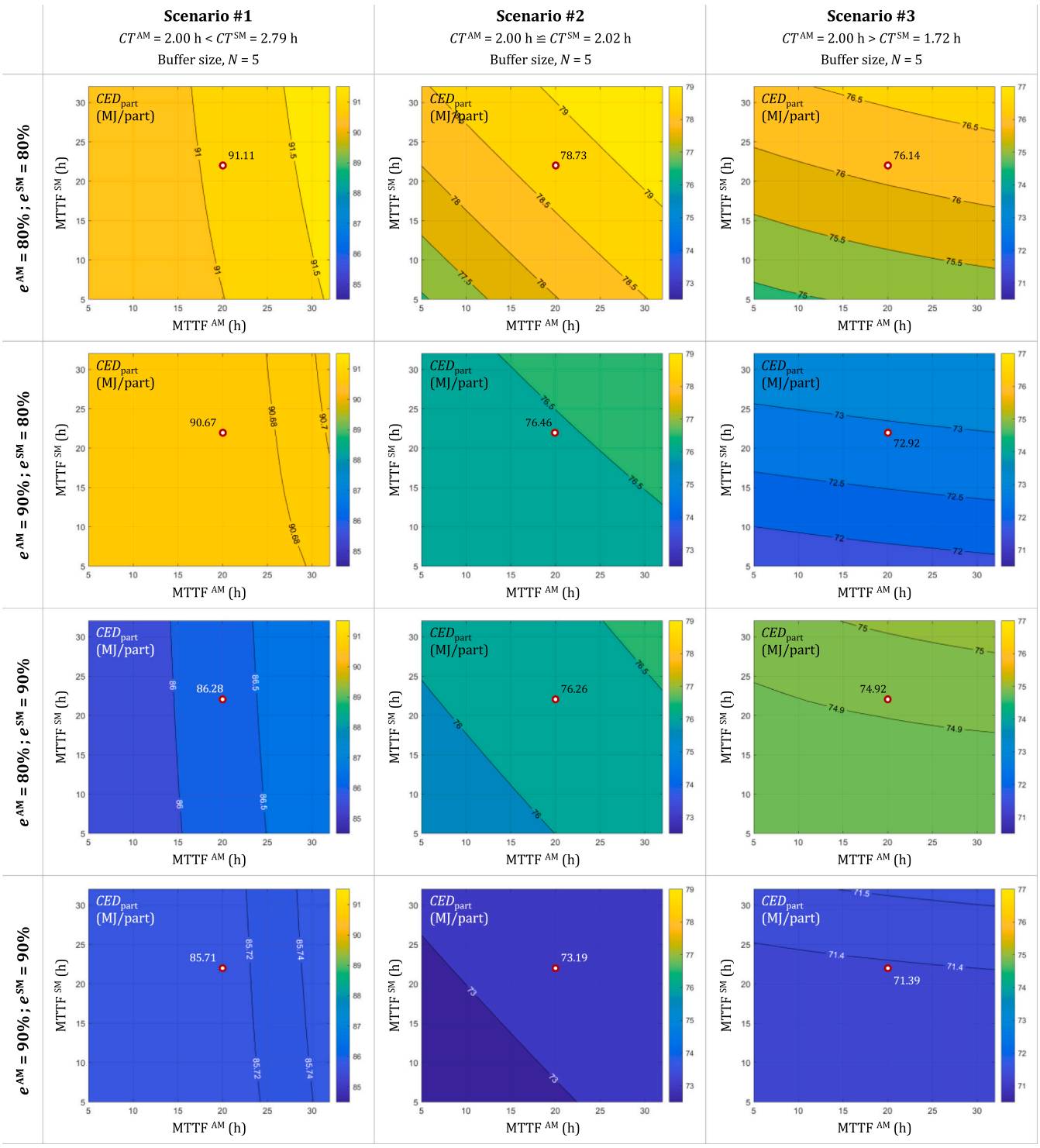

Fig. 8. Results of the sensitivity analysis performed on CED_{part} (in MJ/part) with respect to variations in $MTTF^{k}$ and efficiency levels (e^{k}) of the additive (AM) and subtractive (SM) stages.

bottleneck in idle states decreases. Finally, the effect of improving the *MTTR* while keeping the same *MTTF* on the performance metrics can be observed. For example, consider Scenario 2. When $e^{AM} = 80$ % and $MTTF^{AM} = 20$ h, $MTTR^{AM} = 5$ h. When $MTTF^{AM} = 20$ h and $e^{AM} = 90$ %, $MTTR^{AM}$ decreases to 2.22 h, corresponding to a ~50 % improvement. This improvement in *MTTR* for the AM stage leads to a reduction of 2.2 MJ/part in CED_{part} (from 78.7 to 76.5 MJ/part) and an increase of 0.02 part/h in throughput (from 0.37 to 0.39 part/h). By contrast, a 50 % reduction in $MTTF^{AM}$ (from 20 h to 10 h) results in only a minor reduction of 0.4 MJ/part in CED_{part} (from 78.7 to 78.3 MJ/part) and a negligible change in throughput (less than 0.0001 part/h). These results confirm the significant impact of non-productive times due to stochastic system dynamics on the performance metrics, particularly on CED_{part}.

The contribution of consumables, as also reported in previous studies, represents a limited share of the overall environmental impact. As shown in Fig. 4, their contribution to CED_{part} accounts for approximately 13–14 % of the total in Scenario 1 and 15–16 % in Scenarios 2

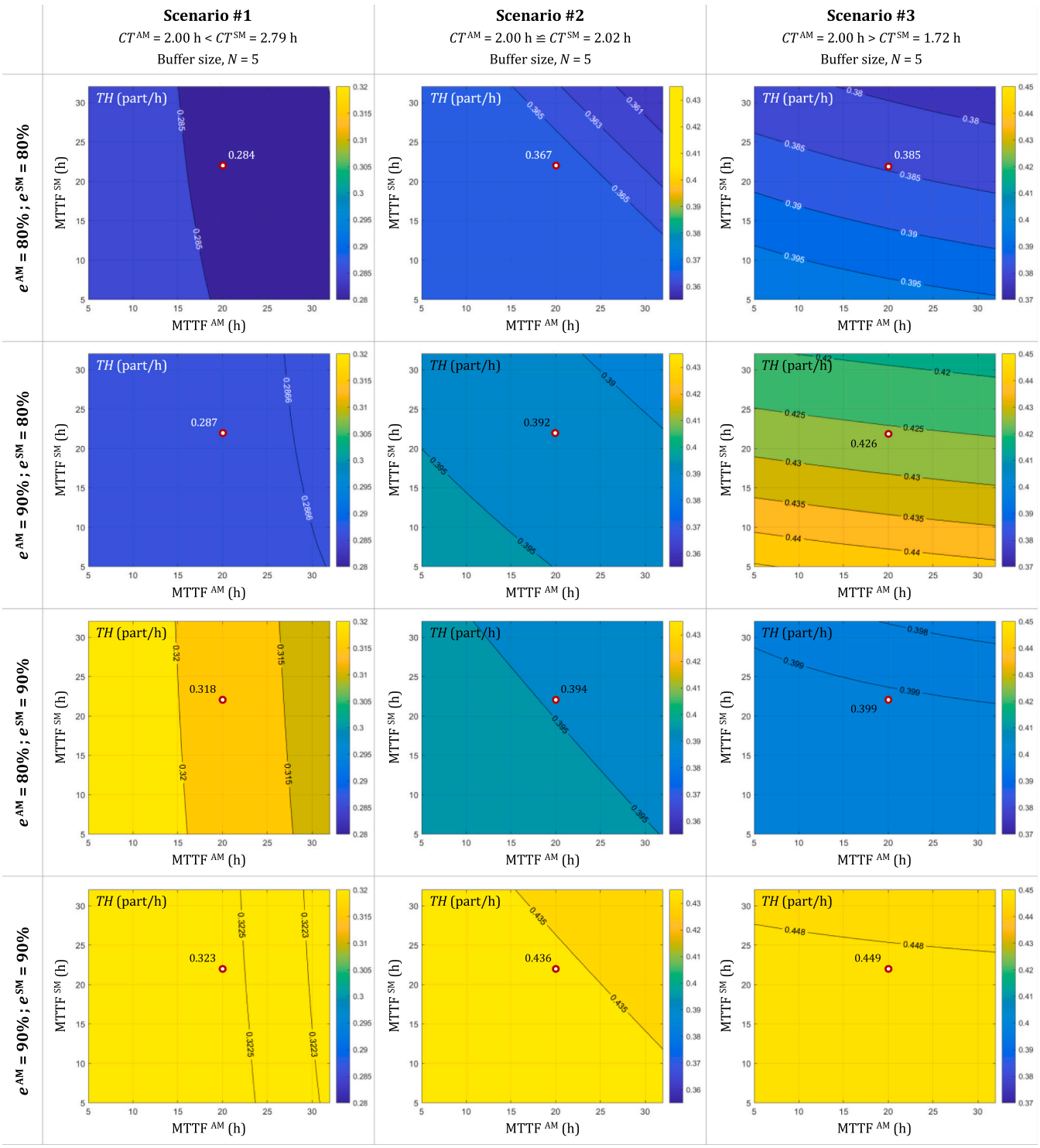

Fig. 9. Results of the sensitivity analysis performed on throughput (in part/h) with respect to variations in $MTTF^k$ and efficiency levels (e^k) of the additive (AM) and subtractive (SM) stages.

and 3. According to the modeling assumptions (refer to Eq. 13), this contribution remains constant and invariant across system configurations and scenarios. If different impact contributions were considered, this would result in an upward (for higher impacts) or downward (for lower impacts) shift of the curves in Figs. 5 and 7, without altering the observed trends or the discussion of the results.

5. Conclusions and outlook

Hybrid manufacturing systems combine additive and subtractive unit processes within an integrated workflow, aiming to leverage the strengths of each technology, such as the flexibility and higher material utilization efficiency of additive manufacturing, and the dimensional accuracy and surface finish quality of subtractive operations. This study presents a framework for evaluating the environmental performance of hybrid manufacturing systems, considering both system configuration

and variations in process parameters. Unlike traditional approaches that assess energy use and emissions in isolation at the process level, the proposed method incorporates system-level interactions (such as blocking and starvation effects) arising from the coupling of additive and subtractive stages. Buffer capacity is also included as a decision variable within the model. While the methodology builds upon well-established approaches (Markov chain modeling, empirical LCA-based metrics) and can be considered incremental from a methodological perspective, its main strength lies in the integration of system-level dynamics, process strategies, and environmental assessment within a unified and systematic methodology. The proposed approach advances beyond traditional DES, LCA-based, and reinforcement learning methods. It enables the evaluation of environmental impacts for alternative system configurations and process parameters, capturing system-level interactions based on stochastic dynamics that are typically overlooked in process-level LCA. Moreover, it allows the definition of explicit relationships between productivity and sustainability metrics and the configuration parameters, without the high data or computational demands of DES or reinforcement learning (RL) approaches. Indeed, this approach is suitable for the configuration phase of manufacturing systems, where production data is not usually available, and data-driven methodologies such as RL may rely on synthetic-generated data based on the same assumptions used in this work. Similarly, DES provides equivalent results, albeit with substantially higher computational requirements. Therefore, the proposed framework supports sustainability-oriented process planning and can be readily applied in industrial contexts due to its relatively low computational effort.

The methodology was applied to a case study involving WAAM followed by finish machining (i.e., 5-axis CNC milling) for the production of a steel component. Three scenarios were analyzed, in which the milling process was slower than, approximately equal to, or faster than the AM process. Numerical results show that environmental performance is influenced by system-level interactions as well as system configurations. Increasing buffer capacity generally reduces the occurrence of non-productive states and enables the system to operate closer to its theoretical throughput. As throughput increases, both energy consumption and emissions per part tend to decrease. This trend aligns with existing process-level studies that report an inverse relationship between specific energy consumption and production rates, while extending the analysis to a multi-stage system context. Overall, the results highlight that environmental performance depends not only on the efficiency of individual processes, but also on system configuration and dynamic interactions across stages.

Despite the potential relevance of the findings, this study has some limitations that suggest directions for future work. The model relies on analytical formulations and empirical parameters, simplifying some of the aspects of industrial systems. Each unit process was described using only two states (productive or failed), based on average values such as *MTTF*, *MTTR*, and *CT*. While this supports analytical tractability, more detailed process dynamics could improve accuracy, as the use of switch on/off policies where feasible. Using assumed rather than experimentally measured parameters introduces limitations, which have been explicitly acknowledged. Also, the modeling of unit processes based on a Markovian representation relies on the assumption of exponential distributions for state transitions. Although this assumption may appear restrictive, it can be relaxed by employing Phase-Type (PH) distributions, which allow mapping empirical statistical distributions of times into Markovian states, thus generalizing the applicability of the proposed approach to experimental data. For future developments, validation could be strengthened by acquiring primary experimental data for both the additive and subtractive stages, including machine efficiency, consumable usage, and process reliability metrics. This would enhance the robustness of the predictive outcomes.

Moreover, the impact of process parameters on product quality was not considered, which may be justified for WAAM, where energy input is more sensitive to parameter variation than microstructural outcomes [9], but not necessarily for other technologies. In the subtractive stage, aspects like tool wear affecting minor stoppages were also omitted, though they could be integrated using Taylor's equation [47]. Also, extending the model to other AM-based processes would require adjustments in productivity and energy calculations. The current model has been applied to a WAAM+CNC system, where production proceeds one part at a time, allowing a straightforward calculation of throughput, energy consumption, and CO_2 emissions per part. Extending the methodology to a PBF+CNC system or other batch-oriented additive processes would introduce additional complexities, as multiple parts may be built simultaneously within the same AM job (stacking) to optimize the use of the build volume. Environmental metrics must then account for total batch consumption and emissions, which need to be allocated to the individual parts. Furthermore, while WAAM+CNC follows a largely linear workflow, PBF+CNC requires scheduling CNC operations across multiple parts from the same AM-ed batch, potentially introducing buffer constraints, additional idle times, and stochastic interactions. Accurately modeling such systems would require the framework to incorporate batch production dynamics, account for variability in part-level process times and resource allocation, and introduce additional states or transition rules in the analytical model to capture scheduling effects on throughput and system-level interactions. Despite these challenges, the conceptual framework remains applicable and could serve as an evaluation kernel for future extended studies. Overall, future developments should include validation with other industrial data or processes, simulation-based enhancements, and the addition of indicators such as material yield, cost, and compliance rate. Integration with multi-objective optimization could further support sustainability-oriented decision-making.

CRediT authorship contribution statement

Maria Chiara Magnanini: Writing – review & editing, Writing – original draft, Validation, Software, Methodology, Investigation, Formal analysis, Conceptualization. **Paolo C. Priarone:** Writing – review & editing, Writing – original draft, Visualization, Validation, Resources, Methodology, Investigation, Conceptualization.

Declaration of Competing Interest

The authors declare that they have no known competing financial interests or personal relationships that could have appeared to influence the work reported in this paper.

One of the authors (M.C. Magnanini) is an Editorial Board Member (Reviewer Board) for CIRP Journal of Manufacturing Science and Technology and was not involved in the editorial review or the decision to publish this article.

Acknowledgments

P.C. Priarone acknowledges the support received from the FACILE project (ID: 765–260), funded by the Piedmont Region (Italy) under the program P.R. F.E.S.R. 2021/27 – D.G.R. n.19–6962 of 29/05/2023 – D. D. n.320/A1907A of 25/07/2023 – Bando SWIch: Support of the Whole Innovation Chain – Action I.1i.1. The authors also gratefully acknowledge the partnership of LMN S.r.l. for conducting the experimental trials.

References

[1] Alaouchiche Y, Ouazene Y, Yalaoui F. Energy-efficient buffer allocation problem in unreliable production lines. Int J Adv Manuf Technol 2021;114:2871–85. https://doi.org/10.1007/s00170-021-06971-1.

[2] AlGeddawy T, ElMaraghy H. Design for energy sustainability in manufacturing systems. CIRP Ann Manuf Technol 2016;65:409–12. https://doi.org/10.1016/j.cirp.2016.04.023.

[3] Ashby MF. Materials and the Environment: Eco-Informed Material Choice, Third Edition. Butterworth Heinemann/Elsevier. 2021. https://doi.org/10.1016/C2016-0-04008-1.

[4] Bandari Y.K., Williams S.W., Ding J., Martina F. Additive manufacture of large structures: Robotic or CNC systems? In: Proc. 26th Annu. Int. Solid Freeform Fabr. Symp. - Addit. Manuf. Conf., August 10-12, 2015. Austin, Texas, USA, pp.17-25.
[5] Behrendt T, Zein A, Min S. Development of an energy consumption monitoring procedure for machine tools. CIRP Ann Manuf Technol 2012;61(1):43–6. https://doi.org/10.1016/j.cirp.2012.03.103.
[6] Bekker ACM, Verlinden JC. Life cycle assessment of wire + arc additive manufacturing compared to green sand casting and CNC milling in stainless steel. J Clean Prod 2018;177:438–47. https://doi.org/10.1016/j.jclepro.2017.12.148.
[7] Campatelli G, Montevecchi F, Venturini G, Ingarao G, Priarone PC. Integrated WAAM-subtractive versus pure subtractive manufacturing approaches: an energy efficiency comparison. Int J Precis Eng Manuf Green Technol 2020;7:1–11. https://doi.org/10.1007/s40684-019-00071-y.
[8] Campatelli G, Venturini G, Grossi N, Baffa F, Scippa A, Yamazaki K. Design and testing of a WAAM retrofit kit for repairing operations on a milling machine. Machines 2021;9(12):322. https://doi.org/10.3390/machines9120322.
[9] Catalano AR, Tebaldo V, Priarone PC, Settineri L, Faga MG. CMT deposition of stainless steel: effects of process parameters on energy demand and microstructure. Prog Addit Manuf 2025;10:6993–7013. https://doi.org/10.1007/s40964-025-01022-7.
[10] Dahmus J.B., Gutowski T.G. An environmental analysis of machining. In: Proc. IMECE ASME Int. Mech. Eng. Congr. RD&D Expo, November 13-19, 2004. Anaheim, California, USA, p. 10.
[11] Ding D, Pan Z, Cuiuri D, Li H. A multi-bead overlapping model for robotic wire and arc additive manufacturing (WAAM). Robot Comput Integr Manuf 2015;31:101–10. https://doi.org/10.1016/j.rcim.2014.08.008.
[12] Duflou JR, Sutherland JW, Dornfeld D, Herrmann C, Jeswiet J, Kara S, et al. Towards energy and resource efficient manufacturing: a processes and systems approach. CIRP Ann Manuf Technol 2012;61(2):587–609. https://doi.org/10.1016/j.cirp.2012.05.002.
[13] European Commission, Directorate-general for research and innovation. Industry 5.0: Towards a sustainable, human-centric and resilient European Industry. Publications Office, 2021. ⟨https://data.europa.eu/doi/10.2777/308407⟩.
[14] European Environment Agency (EEA). Greenhouse gas emission intensity of electricity generation, country level. Available at: ⟨https://www.eea.europa.eu/en/analysis/indicators/greenhouse-gas-emission-intensity-of-1/greenhouse-gas-emission-intensity-of-electricity-generation-country-level⟩ (Published 25 Oct 2024, Modified 27 Jun 2025, Lastly accessed 18 Jul 2025).
[15] Faulkner W, Badurdeen F. Sustainable value stream mapping (Sus-VSM): methodology to visualize and assess manufacturing sustainability performance. J Clean Prod 2014;85:8–18. https://doi.org/10.1016/j.jclepro.2014.05.042.
[16] Flynn JM, Shokrani A, Newman ST, Dhokia V. Hybrid additive and subtractive machine tools – research and industrial developments. Int J Mach Tools Manuf 2016;101:79–101. https://doi.org/10.1016/j.ijmachtools.2015.11.007.
[17] Frigerio N, Matta A. Analysis on energy efficient switching of machine tool with stochastic arrivals and buffer information. IEEE Trans Autom Sci Eng 2016;13(1):238–46. https://doi.org/10.1109/TASE.2015.2492600.
[18] Frischknecht R, Wyss F, Büsser Knöpfel S, Lützkendorf T, Balouktsi M. Cumulative energy demand in LCA: the energy harvested approach. Int J Life Cycle Assess 2015;20(7):957–69. https://doi.org/10.1007/s11367-015-0897-4.
[19] Ghobakhloo M. Industry 4.0, digitization, and opportunities for sustainability. J Clean Prod 2020;252:119869. https://doi.org/10.1016/j.jclepro.2019.119869.
[20] Gisario A, Kazarian M, Martina F, Mehrpouya M. Metal additive manufacturing in the commercial aviation industry: a review. J Manuf Syst 2019;53:124–49. https://doi.org/10.1016/j.jmsy.2019.08.005.
[21] Gobber FS, Priarone PC, Pennacchio A, Actis Grande M. Effect of inert gas pressure on the properties and carbon footprint of UNS S32760 powders made from waste materials by gas atomization. J Mater Res Technol 2024;33:8814–28. https://doi.org/10.1016/j.jmrt.2024.11.195.
[22] Gutowski T., Dahmus J., Thiriez A. Electrical energy requirements for manufacturing processes. In: Proc. 13th CIRP Int. Conf. Life Cycle Eng. 2006. Leuven, Belgium, pp. 5-11.
[23] Helber S, Kellenbrink C, Südbeck I. Evaluation of stochastic flow lines with provisioning of auxiliary material. Spectrum 2024;46(3):669–708. https://doi.org/10.1007/s00291-023-00737-9.
[24] Jeswiet J, Kara S. Carbon emissions and CES™ in manufacturing. CIRP Ann Manuf Technol 2008;57(1):17–20. https://doi.org/10.1016/j.cirp.2008.03.117.
[25] Kara S, Li W. Unit process energy consumption models for material removal processes. CIRP Ann Manuf Technol 2011;60(1):37–40. https://doi.org/10.1016/j.cirp.2011.03.018.
[26] Karimi S, Kwon S, Ning F. Energy-aware production scheduling for additive manufacturing. J Clean Prod 2021;278:123183. https://doi.org/10.1016/j.jclepro.2020.123183.
[27] Khayyati S, Tan B. Supervised-learning-based approximation method for multi-server queueing networks under different service disciplines with correlated interarrival and service times. Int J Prod Res 2022;60(17):5176–200. https://doi.org/10.1080/00207543.2021.1951448.
[28] Khezri A, Benderbal HH, Benyoucef L. Towards a sustainable reconfigurable manufacturing system (SRMS): multi-objective based approaches for process plan generation problem. Int J Prod Res 2021;59(15):4533–58. https://doi.org/10.1080/00207543.2020.1766719.
[29] Koyuncuoğlu MU. Most important performance evaluation methods of production lines: a comprehensive review on historical perspective and emerging trends. Comput Ind Eng 2024;197:110623. https://doi.org/10.1016/j.cie.2024.110623.
[30] Li W, Kara S. An empirical model for predicting energy consumption of manufacturing processes: a case of turning process. Proc Inst Mech Eng Part B J Eng Manuf 2011;225(9):1636–46. https://doi.org/10.1177/2041297511398541.
[31] Loffredo A, May MC, Schäfer L, Matta A, Lanza G. Reinforcement learning for energy-efficient control of parallel and identical machines. CIRP J Manuf Sci Technol 2023;44:91–103. https://doi.org/10.1016/j.cirpj.2023.05.007.
[32] Ma G, Zhao G, Li Z, Yang M, Xiao W. Optimization strategies for robotic additive and subtractive manufacturing of large and high thin-walled aluminum structures. Int J Adv Manuf Technol 2019;101:1275–92. https://doi.org/10.1007/s00170-018-3009-3.
[33] Ma Z, Gao M, Wang Q, Wang N, Li L, Liu C, et al. Energy consumption distribution and optimization of additive manufacturing. Int J Adv Manuf Technol 2021;116:3377–90. https://doi.org/10.1007/s00170-021-07653-8.
[34] Magnanini MC, Tolio TAM. Performance evaluation of asynchronous two-stage manufacturing lines fabricating discrete parts. CIRP J Manuf Sci Technol 2021;33:488–505. https://doi.org/10.1016/j.cirpj.2021.04.002.
[35] May G, Psarommatis F. Maximizing energy efficiency in additive manufacturing: a review and framework for future research. Energies 2023;16(10):4179. https://doi.org/10.3390/en16104179.
[36] Muscatello G, Tolio T. A Markov chain-based approach to model the variance of times-to-failure and times-to-repair in manufacturing systems. Procedia CIRP 2024;130:1322–6. https://doi.org/10.1016/j.procir.2024.10.246.
[37] Paulista CR, Peixoto TA, de Assis Rangel JJ. Modeling and discrete event simulation in industrial systems considering consumption and electrical energy generation. J Clean Prod 2019;224:864–80. https://doi.org/10.1016/j.jclepro.2019.03.248.
[38] Priarone PC, Campatelli G, Montevecchi F, Venturini G, Settineri L. A modelling framework for comparing the environmental and economic performance of WAAM-based integrated manufacturing and machining. CIRP Ann Manuf Technol 2019;68(1):37–40. https://doi.org/10.1016/j.cirp.2019.04.005.
[39] Priarone PC, Catalano AR, Simeone A, Settineri L. Effects of deposition parameters on cumulative energy demand for cold metal transfer additive manufacturing processes. CIRP Ann Manuf Technol 2022;71(1):17–20. https://doi.org/10.1016/j.cirp.2022.03.022.
[40] Priarone PC, Pagone E, Martina F, Catalano AR, Settineri L. Multi-criteria environmental and economic impact assessment of wire arc additive manufacturing. CIRP Ann Manuf Technol 2020;69(1):37–40. https://doi.org/10.1016/j.cirp.2020.04.010.
[41] Priarone PC, Robiglio M, Settineri L. On the concurrent optimization of environmental and economic targets for machining. J Clean Prod 2018;190:630–44. https://doi.org/10.1016/j.jclepro.2018.04.163.
[42] Rodrigues TA, Duarte V, Miranda RM, Santos TG, Oliveira JP. Current status and perspectives on wire and arc additive manufacturing (WAAM). Materials 2019;12:1121. https://doi.org/10.3390/ma12071121.
[43] Sefene EM, Hailu YM, Tsegaw AA. Metal hybrid additive manufacturing: state-of-the-art. Prog Addit Manuf 2022;7:737–49. https://doi.org/10.1007/s40964-022-00262-1.
[44] Smith S, Schmitz T, Feldhausen T, Sealy M. Hybrid metal additive/subtractive machine tools and applications. CIRP Ann Manuf Technol 2024;73(2):615–38. https://doi.org/10.1016/j.cirp.2024.05.002.
[45] Strong D, Kay M, Conner B, Wakefield T, Manogharan G. Hybrid manufacturing–integrating traditional manufacturers with additive manufacturing (AM) supply chain. Addit Manuf 2018;21:159–73. https://doi.org/10.1016/j.addma.2018.03.010.
[46] Tan B, Karabağ O, Khayyati S. Energy-efficient production control of a make-to-stock system with buffer-and time-based policies. Int J Prod Res 2024;62(16):5809–27. https://doi.org/10.1080/00207543.2023.2298488.
[47] Tolio TAM, Ratti A. Performance evaluation of two-machine lines with generalized thresholds. Int J Prod Res 2018;56(1–2):926–49. https://doi.org/10.1080/00207543.2017.1420922.
[48] Weinert K, Inasaki I, Sutherland JW, Wakabayashi T. Dry machining and minimum quantity lubrication. CIRP Ann Manuf Technol 2004;53(2):511–37. https://doi.org/10.1016/S0007-8506(07)60027-4.
[49] Wójcicki J, Tolio T, Bianchi G. Cross-level model of a transfer machine energy demand using a two-machine generalized threshold representation. J Manuf Syst 2021;58:44–58. https://doi.org/10.1016/j.jmsy.2020.11.011.
[50] Yelles-Chaouche AR, Gurevsky E, Brahimi N, Dolgui A. Reconfigurable manufacturing systems from an optimisation perspective: a focused review of literature. Int J Prod Res 2021;59(21):6400–18. https://doi.org/10.1080/00207543.2020.1813913.
[51] Zhao X, Li C, Chen X, Cui J, Cao B. Data-driven cutting parameters optimization method in multiple configurations machining process for energy consumption and production time saving. Int J Precis Eng Manuf Green Technol 2022;9(3):709–28. https://doi.org/10.1007/s40684-021-00373-0.